Copper-Vapor-Assisted Chemical Vapor Deposition for High-Quality and Metal-Free Single-Layer Graphene on Amorphous SiO_2 Substrate

Hyungki Kim,[†,∥] Intek Song,[†,∥] Chibeom Park,[†] Minhyeok Son,[†] Misun Hong,[†] Youngwook Kim,[‡] Jun Sung Kim,[‡] Hyun-Joon Shin,[§] Jaeyoon Baik,[§] and Hee Cheul Choi[†,*]

[†]Department of Chemistry, [§]Pohang Accelerator Laboratory, and [‡]Department of Physics, Pohang University of Science and Technology (POSTECH), San 31, Hyoja-Dong, Nam-Gu, Pohang, Korea 790-784. [∥]These authors contributed equally to this work.

ABSTRACT We report that high-quality single-layer graphene (SLG) has been successfully synthesized directly on various dielectric substrates including amorphous SiO_2/Si by a Cu-vapor-assisted chemical vapor deposition (CVD) process. The Cu vapors produced by the sublimation of Cu foil that is suspended above target substrates without physical contact catalyze the pyrolysis of methane gas and assist nucleation of graphene on the substrates. Raman spectra and mapping images reveal that the graphene formed on a SiO_2/Si substrate is almost defect-free and homogeneous single layer. The overall quality of graphene grown by Cu-vapor-assisted CVD is comparable to that of the graphene grown by regular metal-catalyzed CVD on a Cu foil. While Cu vapor induces the nucleation and growth of SLG on an amorphous substrate, the resulting SLG is confirmed to be Cu-free by synchrotron X-ray photoelectron spectroscopy. The SLG grown by Cu-vapor-assisted CVD is fabricated into field effect transistor devices without transfer steps that are generally required when SLG is grown by regular CVD process on metal catalyst substrates. This method has overcome two important hurdles previously present when the catalyst-free CVD process is used for the growth of SLG on fused quartz and hexagonal boron nitride substrates, that is, high degree of structural defects and limited size of resulting graphene, respectively.

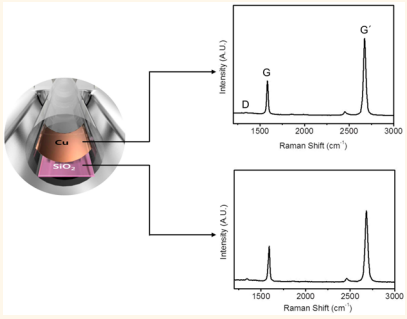

KEYWORDS: graphene · copper vapor · dielectric substrates · chemical vapor deposition

Graphene is an ideal two-dimensional material backboned with sp^2-hybridized carbon atoms and draws significant interest due to its superior electrical properties represented by its high carrier mobility.[1−3] Since its first isolation by mechanical exfoliation,[4,5] large-scale production of graphene has been one of the urgent issues, so various approaches have been attempted, such as epitaxial growth from silicon carbide,[6] chemical reduction of graphene oxide,[7] and chemical vapor deposition (CVD) on transition metal substrates.[8−11] Among these, the CVD process takes special attention as it guarantees high-quality single-layer graphene (SLG) in large size with high yield when proper metal catalyst is employed under specific reaction environments.[12] Besides the size of the graphene layer, the size of each single-crystal domain of SLG can be controlled during the CVD process by modulating nucleation density on a catalyst metal substrate.[13]

The important issue of the metal-catalyzed CVD process is the chemical and physical damage caused during the transfer process that is generally required to fabricate the grown graphene into electronic devices on various dielectric substrates. The transfer process is not just inconvenient but, more importantly, it degrades graphene as wrinkles and cracks are frequently created.[14] Moreover, the metals and supporting polymers that are not completely removed during the removal process also damage or unintentionally alter the intrinsic property of graphene. To avoid these issues, two synthetic strategies have been proposed for the direct formation of graphene on dielectric substrates: (1) by using minimal thin metal catalyst film that is removed during the CVD process[15] and (2) direct growth of graphene on highly

* Address correspondence to choihc@postech.edu.

Received for review November 20, 2012 and accepted July 19, 2013.

Published online July 19, 2013
10.1021/nn402847w

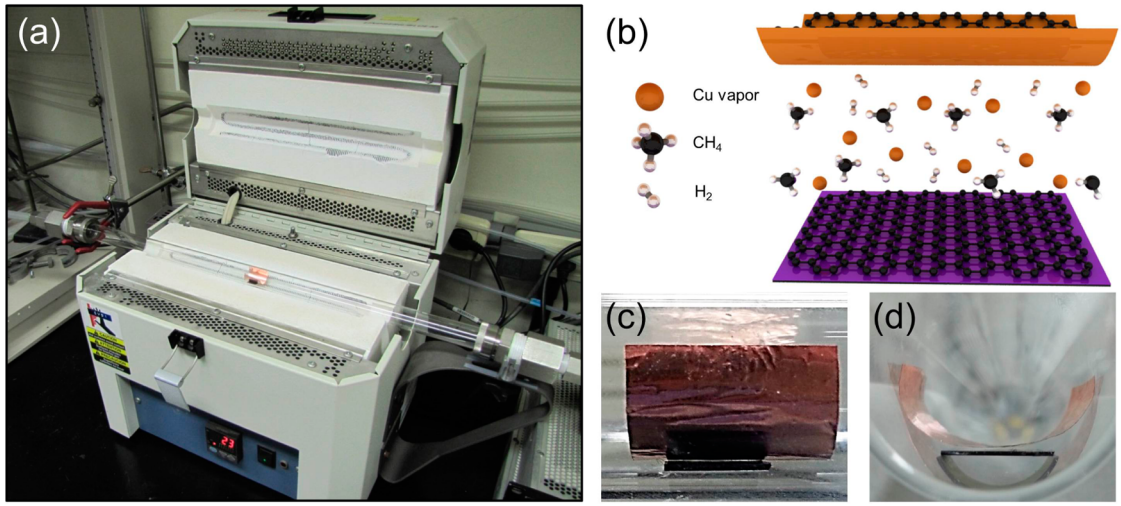

Scheme 1. (a) Photograph and (b) scheme of Cu-vapor-assisted CVD process inducing Cu-vapor-assisted growth of graphene on both Cu foil and underneath the SiO_2/Si substrate. (c,d) Photographs showing side and front views of installed Cu foil and SiO_2/Si substrate, respectively.

crystalline dielectric substrates in a completely metal-catalyst-free environment.[16−18] The use of thin metal catalyst deposited on a dielectric substrate somewhat guarantees the quality of graphene to a certain degree. However, inevitable residual metal still causes contamination on graphene. In the case of metal-catalyst-free growth, as-grown graphene is free from impurities but the graphene contains non-negligible defects due to insufficient pyrolysis of precursor gases and low catalytic activity of dielectric materials. For example, as we have recently demonstrated, graphene synthesized by metal-free CVD process on a single-crystal α-Al_2O_3 wafer yields large-scale SLG, but the populations of wrinkles and ripples are high,[19] while a similar attempt made on an exfoliated h-BN results in graphene pads that have quite limited size.[20] More importantly, apart from the defect and size issues, the metal-free CVD process is not applicable to amorphous dielectric substrates.

One potential method to increase the quality of resulting graphene while minimizing the usage of metal catalyst is to introduce catalyst metal as a vapor that would react with carbon precursor gases in the gas phase as well as on the surface of the substrate. This idea has been recently demonstrated by Teng *et al.* as they report the formation of single- to few-layer graphene on amorphous oxide substrates.[21] However, there is still much room for improvement, especially regarding substantial amounts of defects and nonuniform graphene layers owing to the insufficient catalytic reaction and inhomogeneous nucleation. To the best of our knowledge, it has not been demonstrated yet that exclusive SLG can be grown on amorphous substrates, of which quality in terms of degree of defect and size is still comparable to the one grown on metal catalyst.

Herein we report that high-quality and large-size (up to 1 mm^2) SLG is directly synthesized on various nonmetal substrates including amorphous SiO_2/Si by using remotely provided Cu vapor during the CVD. The optimized amount of Cu vapor is supplied from a Cu foil suspended on top of a substrate without physical contact. Raman spectroscopy and atomic force microscopy (AFM) studies have confirmed that the resulting graphene has a single layer with very low degree of sp^3-type structural defect, small population of wrinkles. The as-grown graphene is confirmed to be free of Cu residue, as Cu is not detected by synchrotron X-ray photoelectron spectroscopy (XPS). The charge carrier mobility of as-grown graphene is similar to the value measured from the graphene grown on Cu foil by a regular CVD process. We also demonstrate that our method is applicable to arbitrary substrates (h-BN and quartz).

RESULTS AND DISCUSSION

The Cu-vapor-assisted SLG growth was performed in a horizontal tube type vacuum CVD system (Scheme 1). A SiO_2/Si substrate was located at the center of the quartz tube, above which a piece of rolled Cu foil is suspended, avoiding physical contact between the foil and substrate. We confirmed that the Cu foil was not in contact with the substrate by monitoring the Cu-free clean surface of the SiO_2/Si substrate after the reaction using an optical microscope as well as by analyzing the surface using a synchrotron XPS (*vide infra*). If they were in contact, the Cu−Si alloy formation reaction would rapidly occur to result in mechanical damage on both foil and substrate.[22] The generation of Cu vapor at the typical growth temperature of 1000 °C is easily assured by observing Cu vapor deposits at the end zones of the quartz tube (Supporting Information Figure S1). Interestingly, the mobility of Cu vapor turns out to be quite high enough to overcome the gas flow and vacuum forces to travel toward both ends of the tube as the deposits are found not just on the

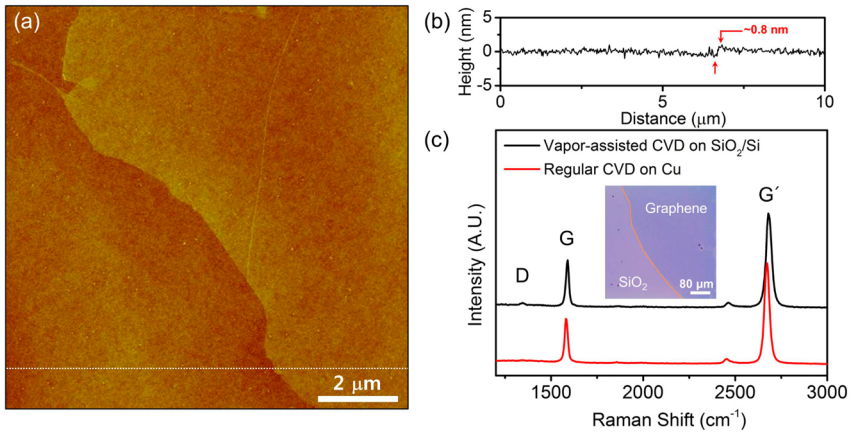

Figure 1. (a) Representative AFM image of SLG grown on SiO_2/Si by Cu-vapor-assisted CVD process. (b) Height profile along the dotted line in (a). (c) Raman spectra corresponding to SLG shown in (a) (black) and transferred SLG on SiO_2/Si after grown on Cu foil (red). The inset in (c) is a bright-field optical microscope image. The yellow line indicates the boundary of SLG and bare SiO_2/Si.

downstream side but also on the upstream side. The fact that the remotely provided Cu vapor indeed involves the growth of graphene was confirmed by testing the same reaction using Ni foil that is known to have much lower vapor pressure ($P_{vapor}^{0} = 6 \times 10^{-10}$ atm)[23] than Cu ($P_{vapor}^{0} = 1 \times 10^{-7}$ atm),[24] by which no graphene was formed (Figure S2).

Representative AFM and bright-field optical images of as-grown graphene on a SiO_2/Si substrate are shown in Figure 1. The AFM image promptly implies that the surface is very flat (R_{rms} = 0.23 nm for wrinkle-free area) and clean without arbitrary particles that are resolved under AFM resolution (Figure 1a). The population of topologically identified wrinkles is significantly lower than the case of graphene transferred from a Cu foil (Figure S3). Such a lowered population of wrinkles seems to be related to the lower thermal expansion coefficient (TEC) difference between graphene ($\sim -1.5 \times 10^{-6}$ °C^{-1})[25] and SiO_2/Si ($\sim 0.4 \times 10^{-6}$ °C^{-1})[26] compared with graphene and Cu ($\sim 24 \times 10^{-6}$ °C^{-1})[27] at 1000 °C as the larger TEC difference is supposed to induce more wrinkles in the resulting graphene.[10,28] The thickness of the graphene measured at the corner region in Figure 1a is 0.8 nm, which agrees well with previously reported data for SLG[5] (Figure 1b). Transmission electron microscopy (TEM) images depicting a single-layer graphene cross section (Figure 2a,b) with a clear hexagonal electron diffraction pattern with monotonous intensities from the equivalent {1100} and {2110} planes further confirm that the graphene is indeed grown in a single layer[29,30] (Figure 2c,d).

Raman spectroscopy further confirms that the Cu-vapor-assisted CVD process produces high-quality SLG with low degrees of structural defects. First, the fact that the synthesized graphene is SLG is confirmed by the $I_{G'}/I_G \approx 1.8$, and the G′ band fitted well to a single Lorentzian shape with full width at half-maximum (fwhm) of 33 cm^{-1} (Figure 1c, black curve). Second, the quality of SLG is confirmed by the low intensity of the D band showing up at 1345 cm^{-1}, indicating the

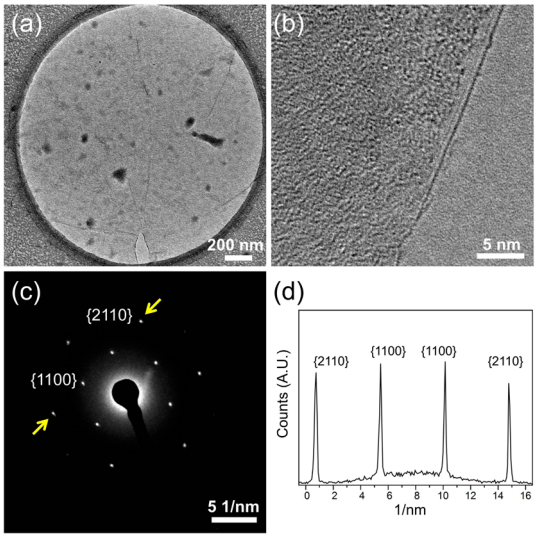

Figure 2. (a) Low-magnification TEM image of transferred as-grown graphene by Cu-vapor-assisted CVD process. (b) High-resolution TEM image of transferred graphene examining the folded region that identifies single-layer graphene. (c) Selected area electron diffraction (SAED) pattern obtained from transferred graphene at normal incidence. (d) Profile plot of diffraction peak intensities across an imaginary line indicated by the yellow arrow.

low population of sp^3-type defect. To compare the quality of as-grown SLG with the SLG grown on Cu foil by regular CVD, we examined the SLG grown on a Cu foil with Raman spectroscopy. Note that the SLG grown on a Cu foil was transferred onto a new SiO_2/Si substrate for Raman study because Cu foil induces high Raman background signal due to surface plasmon emission (Figure S4a). As shown by the red spectrum in Figure 1c, the intensity of the D band, $I_{G'}/I_G \approx 2.1$, and G′ band fitted well to a single Lorentzian shape, and the fwhm of 30 cm^{-1} is highly comparable to those measured from the SLG grown by the Cu-vapor-assisted process. The Cu-vapor-assisted CVD process generates high-quality SLG as large as ~1 mm^2. A bright-field optical microscope image of a large-size

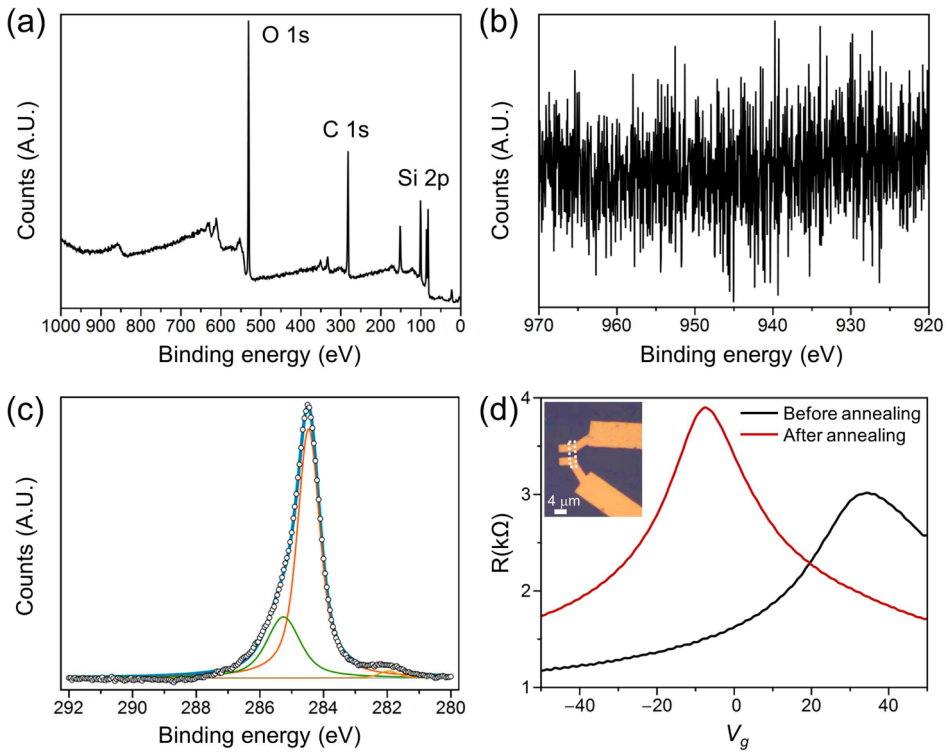

Figure 3. (a) X-ray photoelectron spectroscopy (XPS) survey spectrum. (b) XPS spectrum examined from 945 to 925 eV where the Cu2p$_{3/2}$ peak is supposed to appear. (c) XPS spectrum of C1s. (d) Resistance (R)−gate voltage (V_g) curve of the graphene FET device measured from an as-prepared device (black) and after vacuum annealing at 400 K for 5 min (red). Inset is an optical image of the device, and white box indicates the patterned graphene region.

SLG on a SiO_2/Si is shown as an inset in Figure 1c. The image also shows a clear color contrast between the SLG region and bare SiO_2/Si as marked by a yellow line for clarity. The long-range order uniformity of SLG grown on SiO_2/Si by the Cu-vapor-assisted CVD process is evaluated through Raman mapping for a large area ($45 \times 45\ \mu m^2$). The D, G, and G′ band mapping images show negligible intensity changes throughout the scanned area, indicating that the SLG is highly uniform (Figure S4c−e). The $I_{G'}/I_G$ ratio mapping image shows that the graphene is mostly single layer (>95%) with a small fraction of few-layer graphene flakes (Figure S4f).

The Raman G and G′ bands of the SLG grown by the Cu-vapor-assisted CVD process appear at 1592 and 2686 cm^{-1}, respectively. Compared with the SLG grown by regular CVD on Cu foil of which Raman G and G′ bands appear at 1582 and 2673 cm^{-1}, respectively, the SLG grown by the Cu-vapor-assisted CVD process shows clear blue shifts in both G and G′ bands. This shift seems to be attributed to the compressive strain induced by the difference of thermal expansion coefficients of substrate and graphene.[31]

One of the key conditions that the Cu-vapor-assisted CVD process should meet is that the resulting SLG should be Cu-free. To examine the amount of Cu residue, as-grown SLG on SiO_2/Si was examined by synchrotron XPS. To clarify that there is no formation of copper silicide (Cu_xSi_y) and carbon silicide (SiC) on SiO_2/Si, we used synchrotron XPS at the Pohang Accelerator Laboratory (PAL). To confirm that there is no Cu contamination in graphene, we conducted scanning photoemission microscopy (SPEM) to find the position of graphene grown on SiO_2/Si. As shown in Figure S5a,b (Supporting Information), the red square on the optical image is consistent with the SPEM image mapped with the intensity of C1s peaks. Neither the survey spectra (Figure 3a) nor the magnified spectra for the Cu2p$_{3/2}$ peak region (Figure 3b) shows the presence of Cu residues within the detection limit, while the C1s peak corresponding to the sp^2 carbon is clearly shown at 284.4 eV (Figure 3c). This result indicated that any copper-related chemical species are not observed within the detection limit of high-resolution synchrotron XPS.

In addition, we found the absence of any peaks within the range of 283.2 to 283.6 eV, which corresponds to C1s of the SiC species.[32] In order to analyze the XPS data, we used Shirley background and Gaussian−Lorentzian curves to deconvolute each spectrum. Note that the deconvoluted peak at 285.3 eV may originate from the sp^3 C−C bond at the defects of graphene or the polymer residues from photolithography for the evaporation of gold pads, as shown in Figure S5a.[33] A small peak at 281.9 eV in the C1s spectra is attributed to charging effect because the high-energy X-ray beam is focused on a very small area using a Fresnel zone plate when the SPEM was used. To confirm that the peak at 281.8 eV is related to a

charging effect, the X-ray beam was defocused to reduce the charging effect by decreasing the beam flux (defocusing X-ray beam was done by moving the Fresnel zone plate along the beam axis). The peak at 281.8 eV disappeared in the C1s spectra (Figure S5c).

To investigate the electrical properties, bottom-gated graphene field effect transistor (FET) devices were fabricated using as-grown SLG on SiO_2/Si without any transfer process involved. By employing standard e-beam lithography and thermal metal evaporation, graphene was patterned and Cr/Au electrodes were deposited on the device as it has both channel length and width of 2 μm (inset of Figure 3d). The detailed fabrication process is described in the Experimental Section. A typical electrical transport property of SLG grown by Cu-vapor-assisted CVD process is measured at room temperature where 250 nA is applied between the source and drain electrodes using a standard lock-in technique (Figure 3d). The as-fabricated device shows an ambipolar behavior with its Dirac point shifted toward the positive gate voltage region (black curve). After annealing the device in vacuum for 5 min at 400 K, however, the device recovers its intrinsic property showing $V_{Dirac} \approx 0$ (red curve). Such a large shift of the Dirac point when measured right after fabrication is believed to originate from the residue of the e-beam resist (PMMA). Similar effect showing the Dirac point shift up to 30−40 V that is recovered after vacuum annealing has been reported from the transferred graphene for which PMMA is used as a support during the transfer process.[34,35] From the slope of the transport curve, carrier mobility of the graphene is calculated using an equation of $\mu = 1/C_g(dg_{ds}/dV_g)$, where the μ is the charge carrier mobility, g_{ds} is

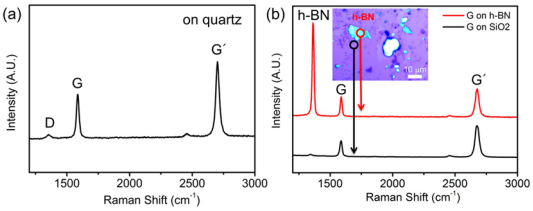

Figure 4. Raman spectra of SLG grown by Cu -vapor-assisted CVD process on (a) α-Al_2O_3 and (b) mechanically exfoliated h-BN substrates. Inset in (b) is an optical image of exfoliated h-BN on SiO_2/Si after the reaction. The strong band at 1370 cm^{-1} in the red spectrum is the E_{2g} mode band of h-BN.

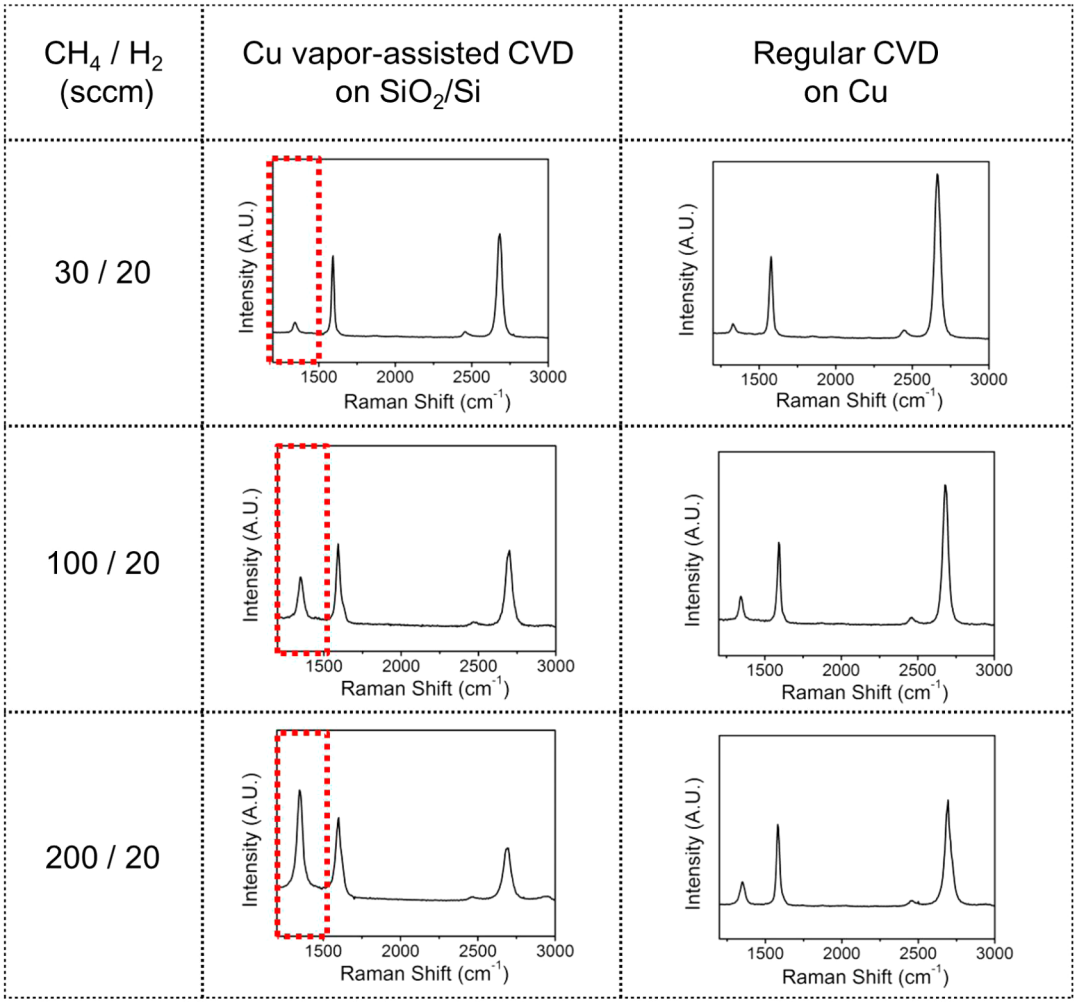

Figure 5. Effect of Cu_{vapor}/CH_4 on the intensity of the D band of graphene. All spectra are normalized by G band intensities.

conductance, and C_g is the gate capacitance. The hole and electron mobilities extracted from this device are about 800 and 700 $cm^2 \cdot V^{-1} \cdot s^{-1}$, respectively, which are similar to those of graphene grown on metal catalysts.[36−38]

One of the advantages of the Cu-vapor-assisted CVD process is that SLG can be formed on arbitrary substrates. To prove the possibility of its generalization, we performed the same reactions on fused quartz and exfoliated h-BN at the same growth condition used for the graphene growth on SiO_2/Si. Figure 4a,b shows Raman spectra of graphene grown on quartz and exfoliated h-BN, respectively. Both spectra show typical characteristic features of SLG as they exhibit $I_{G'}/I_G \approx 1.7$ (quartz) and 1.5 (h-BN) with the G′ band fitted well to a single Lorentzian shape with fwhm of 31 (quartz) and 32 cm^{-1} (h-BN). As indicated by black and red circles in Figure 4b, it is noteworthy that the grown SLG is large enough to fully cover the h-BN surface and bare SiO_2/Si. The successful growth of high-quality and large-scale SLG on both quartz and h-BN is thrilling as the Cu-vapor-assisted CVD process overcomes two main hurdles present in the previous metal-free CVD process, by which only defective SLG and graphene pads with limited size (~150 nm of diameter) were obtained on both α-Al_2O_3[19] and h-BN,[20] respectively.

We believe that the growth mechanism is similar to the one proposed by Teng *et al.*[21] At the growth temperature of 1000 °C, Cu foil is easily evaporated to give off Cu vapor due to its high vapor pressure, which is assured by observing Cu vapor deposit at both ends of the quartz tube, as shown in Figure S1. Then Cu vapor meets methane precursors adsorbed on the substrate surface to nucleate graphene formation, followed by propagation of graphene growth in a lateral direction. The reason for the successful synthesis of high-quality SLG compared with the case reported by Teng *et al.*[21] seems to be attributed primarily to the ideal ratio of Cu vapor to methane gas (Cu_{vapor}/CH_4). To confirm the effect of Cu_{vapor}/CH_4 on the quality of graphene, we performed both Cu-vapor-assisted reactions on SiO_2/Si substrates and regular CVD reactions on Cu foils at various concentrations of methane gas. Note again that the graphene grown on a Cu foil was transferred to a fresh SiO_2/Si substrate for an accurate Raman analysis. In the former case, the intensity of the D band is significantly increased when methane flow is increased, as highlighted by red dotted boxes (Figure 5, left column), while much narrower swing in D band intensity change is observed from the latter case (Figure 5, right column). In detail, the integrated intensity ratio of D band to G band (I_D/I_G) is increased from 0.21 to 0.74 then to 1.33 for the Cu-vapor-assisted CVD process, while the ratios are 0.15, 0.37, and 0.48 for the regular CVD reaction on Cu foil. It should be noted that all the Raman spectra in Figure 5 were taken by averaging 10 000 spectra obtained in $25 \times 25\ \mu m^2$ of each sample to secure the reliability. An important conclusion that can be drawn from these results is that the effect of methane, eventually ruling the Cu_{vapor}/CH_4, is highly critical more for the Cu-vapor-assisted CVD process than for the regular CVD process to secure high-quality SLG.

CONCLUSION

In summary, we have developed a Cu-vapor-assisted CVD process that allows direct synthesis of large-scale SLG on amorphous SiO_2/Si, quartz, and h-BN substrates. The quality of SLG is highly comparable to that of SLG grown on Cu foil in terms of structural defect level as determined by Raman spectroscopy and AFM exhibiting low D band intensity and smooth topological surface with reduced number of wrinkles, respectively. The Cu vapor generated from Cu foil suspended on top of SiO_2/Si is successfully employed as a remotely provided catalyst for the synthesis of high-quality SLG with high reproducibility. It turns out that the ratio of Cu vapor to the amount of methane gas is critical for the successful synthesis of high-quality SLG. Although Cu vapor is involved in the formation of graphene, the resulting SLG does not contain Cu metal, as confirmed by synchrotron XPS. By completely avoiding graphene transfer process, we have demonstrated that the fabrication of a graphene FET device becomes straightforward, which still gives comparable carrier mobilities to those of graphene grown on metal catalysts. The Cu-vapor-assisted CVD can be applied to basically any solid substrate as demonstrated with quartz and h-BN. By utilizing such a versatility of graphene growth on diverse target substrates, we are currently investigating to find an optimum growth condition including the gap distance between suspended Cu foil and underneath the substrate, which will eventually allow controlled growth of more complex structures including vertically stacked graphene layers that are comparable to the recently reported laterally defined SLG−h-BN single-layer heterostructure.[39]

EXPERIMENTAL SECTION

Synthesis of Graphene by Cu-Vapor-Assisted CVD Process. The synthesis was performed using 1 in. tube-type furnace CVD system equipped with a quartz tube to protect samples from direct contact to heating coils.[10] Prior to the synthesis of graphene, a SiO_2/Si (thickness of SiO_2 = 300 nm) substrate was rinsed with acetone and isopropyl alcohol (IPA), and the Cu foil (25 μm thick, 99.8% purity, Alfa Aesar) was immersed in acetic acid for 5 min to remove native copper oxide. The cleaned SiO_2/Si substrate was placed in the quartz tube at the center of the furnace, then Cu foil was rolled up enough to hang on both sidewalls of the quartz tube and suspended on top of the SiO_2/Si substrate (Scheme 1). The estimated gap between the SiO_2/Si substrate and Cu foil is about 50 μm. The reaction was carried out for

30 min at 1000 °C while introducing 30 sccm of CH_4 and 20 sccm of H_2 at a total pressure of ~5 Torr. After reaction was completed, the sample was cooled to room temperature by opening the cover of the furnace under 20 sccm of H_2 at a total pressure of ~2 Torr. For the regular CVD reaction, everything was same except that only a flat piece of cleaned Cu foil was placed inside the quartz tube. For the growth of SLG on quartz and h-BN, a fused quartz wafer and a mechanically exfoliated h-BN on SiO_2/Si were used.

Transfer of SLG Grown on Cu Foil to the SiO_2/Si Substrate. The SLG grown on a Cu foil was spin-coated with poly(methyl methacrylate) (PMMA, 495 PMMA A4, MicroChem). After hardening at 100 °C for 1 min, the PMMA/graphene/Cu foil was floated in a 1 M ferric chloride hexahydrate ($FeCl_3 \cdot 6H_2O$, Sigma Aldrich, 97%) solution to etch out Cu. The resulting PMMA-supported graphene was scooped out from the etchant and rinsed with deionized water several times. Then, the graphene side was placed on a target SiO_2/Si substrate and dried at 90 °C to provide better adhesion between graphene and the substrates. Finally, PMMA was removed by acetone. The transferred graphene was annealed at 300 °C in Ar/H_2 environment for 4 h.

Transfer of SLG Grown on SiO_2/Si Substrate to the TEM grid. PMMA (495PMMA A5, MicroChem) was spin-coated on the SLG grown on the SiO_2/Si substrate at the rate of 500 rpm for 10 sec, followed by 3000 rpm for the next 30 sec. To detach the PMMA/graphene membrane from SiO_2/Si substrate, the sample was immersed in 1 M NaOH aqueous solution for 1 h. The free-standing PMMA-supported graphene was soaked onto fresh DI water to remove remaining NaOH, and this process was repeated at least twice to clean completely. After cleaning, the sample was scooped with a TEM grid (657-200-Cu, Quantifoil). To remove the capping PMMA, PMMA-supported graphene on the TEM grid was dipped in acetone bath for 3 h at room temperature.

Characterization. Morphology of graphene film was investigated by tapping mode atomic force microscopy (AFM, Nanoscope IIIa, Digital Instrument Inc.). Raman spectra and mapping images of graphene films were measured using a WITEC Alpha 300R Raman spectroscope equipped with a 532 nm diode laser. The spatial resolution of the spectrometer was ~250 nm. Laser excitation power was adjusted below 3 mW to prevent potential thermal damage caused by the laser source. X-ray photoelectron spectroscopy (XPS) was carried out at Pohang Accelerate Laboratory (PAL, Beamline 8A1). Using a Fresnel zone plate, X-ray beam (1.1 keV) was focused and irradiated to a sample in an ultrahigh vacuum (2.0×10^{-10} Torr). The electron diffraction pattern and HRTEM image of graphene were acquired using transmission electron microscopy (TEM, JEM-2200FS with image Cs-corrector) in National Center for Nanomaterials Technology (NCNT) at POSTECH.

Fabrication and Measurement of the FET Device. The bottom-gated FET devices were fabricated by a standard electron beam lithography technique. With a graphene grown on SiO_2/Si, the unwanted area of graphene was removed by oxygen plasma etching treatment. Then, source/drain electrode patterns were fabricated with Cr (5 nm)/Au (30 nm). Electrical transport properties of the SLG were measured by the standard lock-in technique in vacuum conditions (~1×10^{-5} Torr) at 300 K. The sample was annealed at 400 K for 5 min in vacuum to improve the contact between the metal electrode and graphene, as well as to remove the residual electroresist on the graphene surface.

Conflict of Interest: The authors declare no competing financial interest.

Acknowledgment. This work was supported by the National Research Foundation of Korea (NRF) grant funded by Ministry of Science, ICT & Future Planning (2012R1A2A1A01003040, 2010-00285, 2013K2A2A4003581, 2013M3C1A3041869), KOSEF through EPB center (2012-00000526). SRC Center for Topological Matter (No. 2011-0030785). We thank Pohang Accelerator Laboratory (PAL) for the use of 8A1 beamline.

Supporting Information Available: Additional figures. This material is available free of charge *via* the Internet at http://pubs.acs.org.

REFERENCES AND NOTES

1. Geim, A. K.; Novoselov, K. S. The Rise of Graphene. *Nat. Mater.* **2007**, *6*, 183–191.
2. Bolotin, K. I.; Sikes, K. J.; Jiang, Z.; Klima, M.; Fudenberg, G.; Hone, J.; Kim, P.; Stormer, H. L. Ultrahigh Electron Mobility in Suspended Graphene. *Solid State Commun.* **2008**, *146*, 351–355.
3. Dean, C. R.; Young, A. F.; Meric, I.; Lee, C.; Wang, L.; Sorgenfrei, S.; Watanabe, K.; Taniguchi, T.; Kim, P.; Shepard, K. L.; *et al.* Boron Nitride Substrates for High-Quality Graphene Electronics. *Nat. Nanotechnol.* **2010**, *5*, 722–726.
4. Novoselov, K. S.; Geim, A. K.; Morozov, S. V.; Jiang, D.; Katsnelson, M. I.; Grigorieva, I. V.; Dubonos, S. V.; Firsov, A. A. Two-Dimensional Gas of Massless Dirac Fermions in Graphene. *Nature* **2005**, *438*, 197–200.
5. Zhang, Y.; Tan, Y.-W.; Stormer, H. L.; Kim, P. Experimental Observation of the Quantum Hall Effect and Berry's Phase in Graphene. *Nature* **2005**, *438*, 201–204.
6. Berger, C.; Song, Z.; Li, X.; Wu, X.; Brown, N.; Naud, C.; Mayou, D.; Li, T.; Hass, J.; Marchenkov, A. N.; *et al.* Electronic Confinement and Coherence in Patterned Epitaxial Graphene. *Science* **2006**, *312*, 1191–1196.
7. Eda, G.; Fanchini, G.; Chhowalla, M. Large-Area Ultrathin Films of Reduced Graphene Oxide as a Transparent and Flexible Electronic Material. *Nat. Nanotechnol.* **2008**, *3*, 270–274.
8. Reina, A.; Jia, X.; Ho, J.; Nezich, D.; Son, H.; Bulovic, V.; Dresselhaus, M. S.; Kong, J. Large Area, Few-Layer Graphene Films on Arbitrary Substrates by Chemical Vapor Deposition. *Nano Lett.* **2009**, *9*, 30–35.
9. Kim, K. S.; Zhao, Y.; Jang, H.; Lee, S. Y.; Kim, J. M.; Kim, K. S.; Ahn, J.-H.; Kim, P.; Choi, J.-Y.; Hong, B. H. Large-Scale Pattern Growth of Graphene Films for Stretchable Transparent Electrodes. *Nature* **2009**, *457*, 706–710.
10. Li, X.; Cai, W.; An, J.; Kim, S.; Nah, J.; Yang, D.; Piner, R.; Velamakanni, A.; Jung, I.; Tutuc, E.; *et al.* Large-Area Synthesis of High-Quality and Uniform Graphene Films on Copper Foils. *Science* **2009**, *324*, 1312–1314.
11. Gao, L.; Ren, W.; Xu, H.; Jin, L.; Wang, Z.; Ma, T.; Ma, L.-P.; Zhang, Z.; Fu, Q.; Peng, L.-M.; *et al.* Repeated Growth and Bubbling Transfer of Graphene with Millimetre-Size Single-Crystal Grains Using Platinum. *Nat. Commun.* **2012**, *3*, 699.
12. Bae, S.; Kim, H.; Lee, Y.; Xu, X.; Park, J.-S.; Zheng, Y.; Balakrishnan, J.; Lei, T.; Kim, H. R.; Song, Y. I.; *et al.* Roll-to-Roll Production of 30-Inch Graphene Films for Transparent Electrodes. *Nat. Nanotechnol.* **2010**, *5*, 574–578.
13. Li, X.; Magnuson, C. W.; Venugopal, A.; Tromp, R. M.; Hannon, J. B.; Vogel, E. M.; Colombo, L.; Ruoff, R. S. Large-Area Graphene Single Crystals Grown by Low-Pressure Chemical Vapor Deposition of Methane on Copper. *J. Am. Chem. Soc.* **2011**, *133*, 2816–2819.
14. Li, X.; Zhu, Y.; Cai, W.; Borysiak, M.; Han, B.; Chen, D.; Piner, R. D.; Colombo, L.; Ruoff, R. S. Transfer of Large-Area Graphene Films for High-Performance Transparent Conductive Electrodes. *Nano Lett.* **2009**, *9*, 4359–4363.
15. Ismach, A.; Druzgalski, C.; Penwell, S.; Schwartzberg, A.; Zheng, M.; Javey, A.; Bokor, J.; Zhang, Y. Direct Chemical Vapor Deposition of Graphene on Dielectric Surfaces. *Nano Lett.* **2010**, *10*, 1542–1548.
16. Rümmeli, M. H.; Bachmatiuk, A.; Scott, A.; Börrnert, F.; Warner, J. H.; Hoffman, V.; Lin, J.-H.; Cuniberti, G.; Büchner, B. Direct Low-Temperature Nanographene CVD Synthesis over a Dielectric Insulator. *ACS Nano* **2010**, *4*, 4206–4210.
17. Zhang, L.; Shi, Z.; Wang, Y.; Yang, R.; Shi, D.; Zhang, G. Catalyst-Free Growth of Nanographene Films on Various Substrates. *Nano Res.* **2010**, *4*, 315–321.
18. Chen, J.; Wen, Y.; Guo, Y.; Wu, B.; Huang, L.; Xue, Y.; Geng, D.; Wang, D.; Yu, G.; Liu, Y. Oxygen-Aided Synthesis of Polycrystalline Graphene on Silicon Dioxide Substrates. *J. Am. Chem. Soc.* **2011**, *133*, 17548–17551.
19. Song, H. J.; Son, M.; Park, C.; Lim, H.; Levendorf, M. P.; Tsen, A. W.; Park, J.; Choi, H. C. Large Scale Metal-Free Synthesis of Graphene on Sapphire and Transfer-Free Device Fabrication. *Nanoscale* **2012**, *4*, 3050–3054.
20. Son, M.; Lim, H.; Hong, M.; Choi, H. C. Direct Growth of Graphene Pad on Exfoliated Hexagonal Boron Nitride Surface. *Nanoscale* **2011**, *3*, 3089–3093.
21. Teng, P.-Y.; Lu, C.-C.; Akiyama-Hasegawa, K.; Lin, Y.-C.; Yeh, C.-H.; Suenaga, K.; Chiu, P.-W. Remote Catalyzation

for Direct Formation of Graphene Layers on Oxides. *Nano Lett.* **2012**, *12*, 1379–1384.
22. Okamoto, H. Cu-Si (Copper-Silicon). *J. Phase Equilib.* **2002**, *3*, 281–282.
23. Johnston, H. L.; Marshall, A. L. Vapor Pressures of Nickel and of Nickel Oxide. *J. Am. Chem. Soc.* **1940**, *62*, 1382–1390.
24. Geiger, F.; Busse, C. A.; Loehrke, R. I. The Vapor Pressure of Indium, Silver, Gallium, Copper, Tin, and Gold between 0.1 and 3.0 bar. *Int. J. Thermophys.* **1987**, *8*, 425–436.
25. Mounet, N.; Marzari, N. First-Principles Determination of the Structural, Vibrational and Thermodynamic Properties of Diamond, Graphite, and Derivatives. *Phys. Rev. B* **2005**, *71*, 205214.
26. Hahn, T. A.; Kirby, R. K. Thermal Expansion of Fused Silica from 80 to 1000 K—Standard Reference Material 739. *AIP Conf. Proc.* **1972**, *3*, 13–24.
27. White, G. K.; Collocott, S. J. Heat Capacity of Reference Materials: Cu and W. *J. Phys. Chem. Ref. Data* **1984**, *13*, 1251–1257.
28. Liu, N.; Pan, Z. H.; Fu, L.; Zhang, C. H.; Dai, B. Y.; Liu, Z. F. The Origin of Wrinkles on Transferred Graphene. *Nano Res.* **2011**, *4*, 996–1004.
29. Lee, S.; Lee, K.; Zhong, Z. Wafer Scale Homogeneous Bilayer Graphene Films by Chemical Vapor Deposition. *Nano Lett.* **2010**, *10*, 4702–4707.
30. Meyer, J. C.; Gein, A. K.; Katsnelson, M. I.; Novoselov, K. S.; Obergfell, D.; Roth, S.; Girit, C.; Zettl, A. On the Roughness of Single- and Bi-layer Graphene Membranes. *Solid State Commun.* **2007**, *143*, 101–109.
31. Yoon, D.; Son, Y. W.; Cheong, H. Negative Thermal Expansion Coefficient of Graphene Measured by Raman Spectroscopy. *Nano Lett.* **2011**, *11*, 3227–3231.
32. Oliveira, M. H., Jr.; Schumann, T.; Fromm, F.; Koch, R.; Ostler, M.; Ramsteiner, M.; Seyller, T.; Lopes, J. M. J.; Riechert, H. Formation of High-Quality Quasi-Free-Standing Bilayer Graphene on SiC(0001) by Oxygen Intercalation upon Annealing in Air. *Carbon* **2013**, *52*, 83–89.
33. Lin, Y. C.; Lu, C. C.; Yeh, C. H.; Jin, C. H.; Suenaga, K.; Chiu, P.-W. Graphene Annealing: How Clean Can It Be? *Nano Lett.* **2012**, *12*, 414–419.
34. Pirkle, A.; Chan, J.; Venugopal, A.; Hinojos, D.; Magnuson, C. W.; McDonnell, S.; Colombo, L.; Vogel, E. M.; Ruoff, R. S.; Wallace, R. M. The Effect of Chemical Residues on the Physical and Electrical Properties of Chemical Vapor Deposited Graphene Transferred to SiO_2. *Appl. Phys. Lett.* **2011**, *99*, 122108.
35. Cheng, Z.; Zhou, Q.; Wang, C.; Li, Q.; Wang, C.; Fang, Y. Toward Intrinsic Graphene Surfaces: A Systematic Study on Thermal Annealing and Wet-Chemical Treatment of SiO_2-Supported Graphene Devices. *Nano Lett.* **2011**, *11*, 767–771.
36. Levendorf, M. P.; Ruiz-Vargas, C. S.; Garg, S.; Park, J. Transfer-Free Batch Fabrication of Single Layer Graphene Transistors. *Nano Lett.* **2009**, *9*, 4479–4483.
37. Liang, X.; Sperling, B. A.; Calizo, I.; Cheng, G.; Hacker, C. A.; Zhang, Q.; Obeng, Y.; Yan, K.; Peng, H.; Li, Q.; *et al.* Toward Clean and Crackless Transfer of Graphene. *ACS Nano* **2011**, *5*, 9144–9153.
38. Song, H. S.; Li, S. L.; Miyazaki, H.; Sato, S.; Hayashi, K.; Yamada, A.; Yokoyama, N.; Tsukagoshi, K. Origin of the Relatively Low Transport Mobility of Graphene Grown through Chemical Vapor Deposition. *Sci. Rep.* **2012**, *2*, 337.
39. Levendorf, M. P.; Kim, C.-J.; Brown, L.; Huang, P. Y.; Havener, R. W.; Muller, D. A.; Park, J. Graphene and Boron Nitride Lateral Heterostructures for Atomically Thin Circuitry. *Nature* **2012**, *488*, 627–632.